Localized delivery and uncaging of glutamate from MRI-visible albumin nanoclusters in the rat hippocampus using focused ultrasound

Megan C. Rich, BA[1], Jennifer Sherwood, PhD[2], Aundrea F. Bartley, PhD[1], W. R. Willoughby, PhD[3], Lynn E. Dobrunz, PhD[1], Farah D. Lubin, PhD[1], Yuping Bao, PhD[2], Mark Bolding, PhD[3,*]

1 Department of Neurobiology, University of Alabama at Birmingham, Birmingham, AL, 35294, USA
2 Department of Chemical and Biological Engineering, University of Alabama at Tuscaloosa, Tuscaloosa, AL, 35487, USA
3 Department of Radiology, University of Alabama at Birmingham, Birmingham, AL, 35294, USA

[*]mbolding@uab.edu

Abstract

Neuropharmacological manipulations have been crucial for advancing fundamental neuroscience and elucidating the relationship between neurotransmitter function, channel kinetics, cellular signaling and behavior. However, systemic delivery of neuropharmacological agents can produce off-target effects that outweigh clinical benefit and confound preclinical results, preventing such interventions from reaching their full potential as therapeutic drugs and tools for research. Localization to specific brain regions requires injections, cannulae, pumps, or other invasive methods that can damage tissue and complicate or prevent translation to humans. Focused ultrasound (FUS) mediated blood-brain barrier (BBB) opening (BBBO) can deliver agents to specific brain regions non-invasively without damaging tissue. FUS can be targeted anywhere in the brain to open the BBB with high spatial resolution, but the use of BBB impermeable agents for localized delivery lacks temporal control, and circulating drugs can still cause systemic effects. Encapsulation of drugs prevents them from acting in non-target areas, and release from the capsules can provide temporal control. Here we demonstrate that MRI visible, albumin-based nanoclusters (NCs) can be used to encapsulate neuromodulators for non-invasive delivery to target rat brain regions via FUS facilitated BBBO. Glutamate and NBQX showed a very low baseline release rate from IV injected NCs. The NCs diffused locally into the brain with FUS facilitated BBBO and provided enhanced MRI contrast at the delivery site. Drug release into brain tissue was triggered by a second FUS treatment (FUS-release) using different parameters from the FUS used for BBBO. Furthermore, FUS-release caused a change in MRI contrast and provided in vivo confirmation of drug release. Using FUS, dye was locally released from NCs 30 minutes after delivery and release of dye into target brain regions was observed 24 hrs after delivery. The drug loading capacity of the NCs was sufficient for inducing localized changes in neural activity in response to glutamate release from NCs in vivo.

Introduction

Neurological disorders such as autism spectrum disorder, schizophrenia, bipolar disorder, and ADHD cannot be completely replicated in animal models, which leads to challenges when attempting to understand their etiology as well as challenges when translating treatment strategies from animal models to humans. Such challenges persist due to underlying mechanisms that are unique to human neurological disorders, and current clinical tools have limited capabilities to resolve this problem[1]. In order to fully understand and treat disorders unique to the human brain, non-invasive, spatiotemporally specific methods for studying interactions between pharmacology and neurophysiology are required that are usable in humans [1]. Lesion studies and clinical pharmacological manipulations have proven to be two of the most powerful tools in modern neuroscience [1–3]. Lesion studies have provided invaluable information about functional localization, but difficulty finding appropriate human subjects makes research slow and expensive. Pharmacological studies have provided important discoveries about endogenous and exogenous chemical-neuronal interactions, but systemic drug delivery can cause confounding effects that may lead to erroneous results. An ideal tool for human neuromodulation studies would provide a non-invasive way to explore location-specific and chemical-specific brain functions, and could be used in combination with functional neuroimaging in the healthy human brain.

As a step toward such a non-invasive neuromodulation technique for use in humans, we have developed a new method in rodents based on a combination of tools that are already used in humans. We combine focused ultrasound (FUS) blood brain barrier (BBB) opening and albumin-based drug carriers that are MRI-visible to achieve targeted drug delivery to the brain. FUS has gained attention as a tool for focal BBB opening (BBBO) [4–10], and can penetrate the skull to safely open the BBB at specific locations [5,11–16]. It is an ideal tool for focal drug delivery due to its current use in humans [17,18] and its non-invasive nature [19,20]. However, brain localization of systemically delivered agents requires that they do not readily cross the BBB and systemic delivery of drugs can cause off target side effects. Albumin based drug carriers have been studied as small molecule carriers to increase drug solubility and control systemic distribution [21,22]. However, the use of albumin drug carriers for localized drug delivery to the brain has yet to be thoroughly investigated. Also, other studies have suggested that they may be sensitive to US triggered destruction [23,24], releasing their contents and providing an element of temporal control. We have shown previously that albumin-based nanoclusters (NCs) can be embedded with ultrasmall iron oxide nanoparticles (USNPs) to provide MRI visibility and can encapsulate dye molecules as well as antibodies [25]. Furthermore, NC load remained inside the NC unless digested with trypsin, and in vivo, NCs remained stable for up to 24 hours [25,26]. Here, we investigated whether albumin-based NCs could be delivered to the rat hippocampus via MRI guided transcranial FUS BBBO for localized drug delivery. We report that NCs can encapsulate the neuromodulatory drugs glutamate and NBQX, and we show that IV injected NCs in vivo can locally diffuse into the brain with FUS facilitated BBBO. The NCs are MRI visible and provide independent confirmation of the site of drug delivery. NCs are also stable in circulation, and once delivered to target brain regions, we were able to induce drug and dye release by a second FUS treatment. The release of glutamate from NCs in vivo caused local neuronal activation demonstrating that the drug loading capacity of the NCs is sufficient for inducing localized changes in neural activity with temporal control.

Materials and Methods

Nanocluster formation and FUS-induced drug release

NCs were created as described previously [25,26]. Briefly, first tannic acid-coated ultrasmall (¡4 nm) iron oxide nanoparticles were synthesized [26], followed by crosslinking of nanoparticles with bovine serum albumin proteins by the addition of ethanol and glutaraldehyde. The overall size of the nanocluster can be tuned by altering the amounts and rates of ethanol addition. Glutaraldehyde provides surface crosslinking of NCs, which subsequently inhibits further growth and aggregation of BSA NCs. For these studies, NCs between 100nm and 200nm were used at a concentration of 2mg/mL. In order to determine the behavior of the NC and the NC load under FUS exposure, we loaded glutamate or NBQX into 100 nm NCs, and measured the release rate using a colorimetric glutamate assay or NBQX colorimetry before and after FUS exposure in vitro (FUS parameters: 0.30 MPa, 1.1 MHz, 10 ms burst, 1 Hz burst repetition rate, 5 minutes, no microbubbles).

MRI Procedure

Male Sprague Dawley rats weighing 250 - 350 g were obtained from Charles River Laboratories and housed in accordance with UAB Institutional Animal Care and Use Committee (IACUC) guidelines. Animals had free access to water and rat chow, and were maintained on a 12:12 hr light:dark cycle. Prior to FUS BBBO procedures, animals were anesthetized with isoflurane ($2 - 3\%$) and positioned on a transportable 3-D printed rat stereotaxic frame containing an MRI fiducial. Animals remained in the stereotaxic frame throughout the MRI and FUS procedures. T1- and T2-weighted MR images were collected on a 9.4 T Bruker horizontal small bore animal MRI scanner with a custom surface coil prior to FUS procedure (prescan), as well as 15 minutes, 30 minutes, and 1 hour after FUS BBBO. The imaging parameters were set as follows: coronal slices, slice thickness 1.5 mm, gap of 1.5 mm, voxel size of $0.2 \times 0.2 \times 1.5$ mm voxels, 0.5 mm gap, FOV = 85×35 mm. A pneumatic pillow sensor placed under the rat chest and connected through an ERT Control/Gating Module (SA Instruments) was used to monitor the rat's respiratory cycle during imaging. During the prescan, hippocampal or anterior cingulate cortex coordinates were measured in 3 planes from the MRI fiducial which would later be used for FUS targeting.

FUS BBB opening and localized delivery of nanoclusters

Animals were transferred in the stereotaxic frame from the MRI to the ultrasound equipment while maintained under anesthesia. The stereotaxic frame was slid into a 3D printed holder, which allows the animal to remain in a static position under the ultrasound apparatus. Prior to FUS BBBO, a tail vein catheter was inserted and hair was removed from the scalp with Nair. Using an XYZ positioning system (Valmex, Bloomfield, NY) driven by LabVIEW software (National Instruments, Austin TX), a pointer to match the transducer focal distance was touched off on the MRI fiducial in the stereotaxic frame and the coordinates that were gathered during the MRI prescan were used to position the focus of the transducer. A water bath was coupled to the scalp with US gel. The FUS transducer was lowered into the water bath to its target position and animals were then intravenously injected with 1mL/kg of 3% Evans blue dye (EBD) (Sigma Aldrich) which was allowed to circulate for 5 minutes. The animals were then slowly infused (0.2mL/2 mins) with 30μL/kg of Definity (Lantheus Medical Imaging, Billerica, MA) while FUS was applied to the target brain region. The FUS transducer was provided by FUS Instruments, (Toronto, ON, Canada) and the FUS

parameters were as follows: 0.30 MPa, 1.1 MHz, 10 ms burst, 1 Hz burst repetition rate, 2 minute duration. The microbubble infusion and FUS exposure were repeated a second time following a 5 minute gap allowing for the first Definity injection to clear from circulation. Only one hemisphere was targeted with FUS BBBO leaving the other for use as an internal control. Immediately following FUS, animals were injected with either 2mL/kg of unloaded NCs, NCs loaded with FITC dye, NCs loaded with glutamate (5mM/mL, Sigma-Aldrich), 2mL/kg of 5mM/mL glutamate (Sigma-Aldrich) in saline, or 2mL/kg of saline alone.

Release-FUS Procedure

Following the 30 minutes MRI postscan, animals receiving release-FUS were removed from the scanner and transported back to the ultrasound equipment while remaining in the stereotaxic frame. They were again slid into the stereotaxic frame holder which provides the same positioning for the BBBO and release-FUS treatments. A water bath was placed over the scalp coupled with ultrasound gel and the FUS transducer was lowered back to its target coordinate. The animals were again treated with a 2 minute FUS exposure to the same target region using the same ultrasound parameters as stated above but without any microbubble injection. FUS application in the absence of microbubbles does not cause the BBB to open further[27]. This was tested in several animals (data not shown), and it is evident in our degree of EBD staining between groups (Figures 4 and 5). In addition, release-FUS does not cause any cFos activation as seen in our control animals (Figure 5). Following release-FUS exposure the animals remained in the stereotaxic frame and were transported back to the MRI scanner for the 1 hour postscan. Animals that did not receive release-FUS were removed from the scanner following the 30 minute postscan and placed back into the MRI for the 1 hour postscan. All animals remained under isoflurane anesthesia during the entire procedure.

Nanocluster MRI contrast analysis

T_1-weighted MRI images were first loaded into 3DSlicer software (https://www.slicer.org/) [28] for nonuniform intensity normalization using the publicly available N4ITK toolkit [29]. The images were then uploaded into FIJI by ImageJ [30], and using a rat brain atlas for reference, an ROI was drawn around both the FUS targeted and the non-targeted hippocampus. The minimum gray value from 3 ROIs per hemisphere were averaged and the ratio of non-target/target hemisphere values were analyzed.

Brain tissue processing, immunofluorescence imaging and analysis

Animals were sacrificed 2 hours after NC injection which was 1.5 hours after release-FUS. Sacrificed animals were perfused with 4% buffered formalin and brain tissue was immediately collected and frozen in Optimal Cutting Temperature compound (O.C.T.,Tissue-Tek, Sakura Finetek USA). Brain tissue was stored at -80°C until cryostat sectioning. 10μm frozen sections were first thawed at room temperature for 10 minutes then fixed with 4% buffered formalin and washed 3 times with 1X PBS. Sections then underwent antigen retrieval by incubating in boiling sodium citrate solution first for 2 minutes, then exchanged with fresh boiling solution and repeated twice for 5 minutes. Slides were then washed 3 times for 3 minutes in 1x PBS. Next, the sections were incubated in 5% goat serum block (Jackson Immunoresearch, West Grove, PA) for 1 hour at 4°C. Serum block was tapped off each slide and excess liquid was absorbed with a kimwipe. Tissue sections were then incubated in primary antibody to

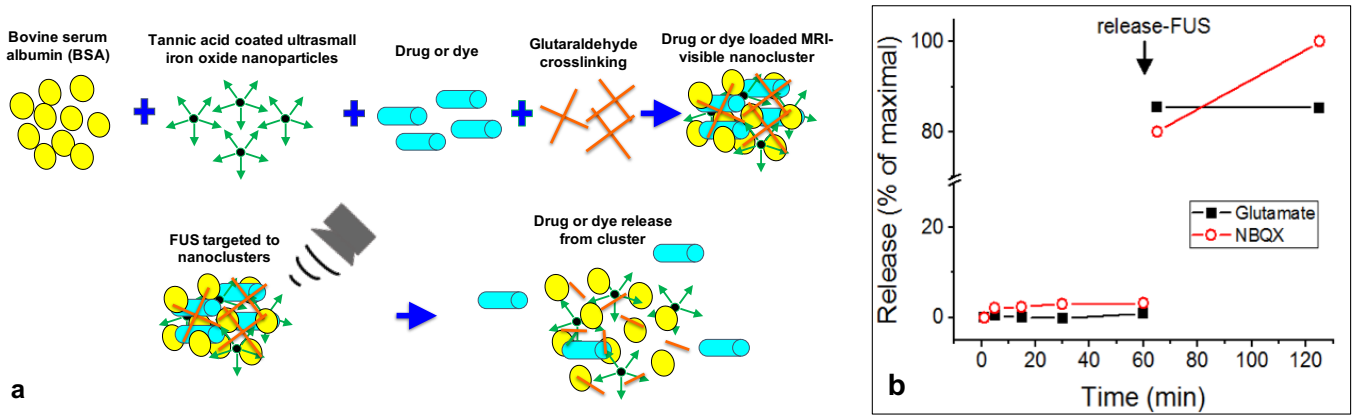

Figure 1. Release-FUS triggers drug release from NCs. (a) Illustration of nanocluster formation and ultrasound triggered release. (b) Glutamate and NBQX colorimetry before and after FUS exposure.

either BSA (1:1000, ThermoFisher, Grand Island, NY) NeuN (1:400 MAB377, MilliporeSigma, St. Louis, MO) or cFos (1:1000, SC-52, Santa Cruz Biotechnology, Dallas, TX) overnight at 4°C followed by rinsing 3 times with 1x PBS. Sections were then incubated in secondary antibody (1:300, Alexa Fluor 488, 1:300 or AffiniPure Mouse Anti-Rat IgG AMCA conjugate, Jackson Immunoresearch) for 2 hours at room temperature. Slides were then rinsed 3 times with 1x PBS and coverslipped with either Fluoromount mounting medium (ThermoFisher, Grand Island, NY) or Vectashield Mounting Medium with DAPI Hardset (Vector Laboratories, burlingame, CA). Fluorescent microscopy imaging was performed using a Zeiss Axio-Imager microscope and processed using FIJI by ImageJ [30]. Presence of FITC dye in tissue was quantified using the particle analysis function in FIJI. For analysis of anti-cFos stained tissue, DAPI fluorescence images were used to get a total cell count using FIJI's analyze particle function, which also generated outlines of cells which were overlaid onto the green channel depicting cFos fluorescence. cFos positive cells were counted using FIJI's "point" tool. Cell counting was performed blinded to treatment condition, and only DAPI positive cell nuclei that overlapped with the green-cFos channel were counted. The percentage of total cells that were cFos positive cells were compared between groups.

Results

Drug encapsulation and release from nanoclusters

We have previously shown that albumin based, MRI-visible NCs can be used to encapsulate the dye Texas red[25]. NCs were stable at pH levels ranging from 5-9 across 7 days and released dye into the supernatant only after enzymatic digestion with trypsin[25]. This shows that NCs can encapsulate drugs and release them upon enzyme exposure. Figure 1a illustrates how drug or dye loaded NCs are formed with BSA, iron oxide NPs, and glutaraldehyde. FUS-induced release of bound agents from NCs is also depicted. To investigate drug release with FUS as well as test baseline stability with different agents, we loaded glutamate or NBQX into 100nm NCs, and measured the release rate using a colorimetric glutamate assay or NBQX colorimetry. Colorimetry data are plotted in Figure 1b as percent released versus time. The baseline release rate is very low for both drugs, and increases dramatically upon exposure to FUS, which was applied after 1 hour. The FUS parameters were as follows: 0.30 MPa, 1.1 MHz, 10 ms

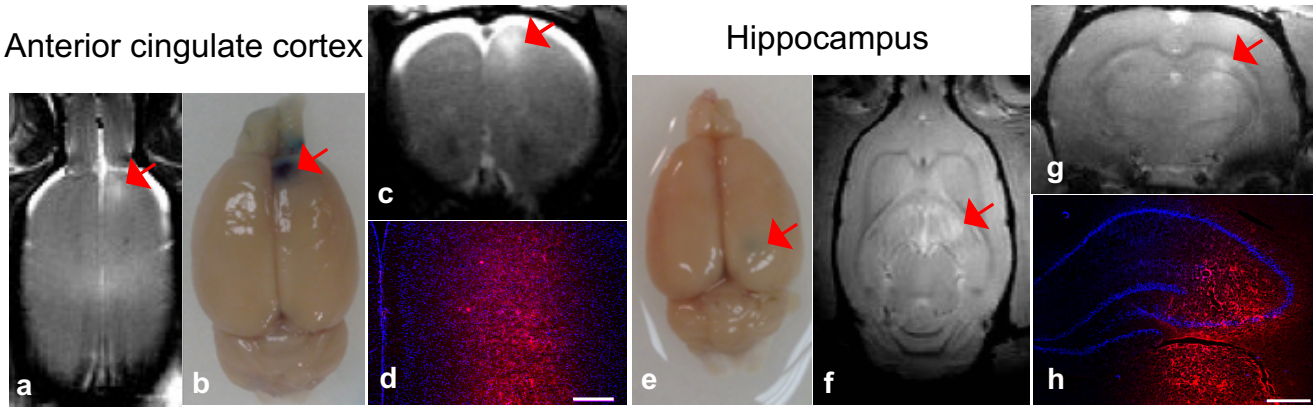

Figure 2. FUS activated focal BBB opening can be targeted to different locations in the rat brain. BBB opening was evident by MRI contrast enhancement (a, c, f and g) and Evans blue dye (EBD) (b, d, e and h) targeted to the anterior cingulate cortex (a-d) and the hippocampus (e-h). FUS parameters: 0.3MPa, 1.1MHz, 10ms burst, 1Hz repetition rate, 120s duration, simultaneous slow infusion of Definity. Scales bars: 500μm (d and h).

burst, 1 Hz burst repetition rate, 5 minutes, no microbubbles. The FUS treatment also resulted in 10% T_1 contrast signal intensity change (data not shown). Based on these data, in the following studies, the NCs were IV injected immediately following BBBO so that the drug load remained inside the NCs as they loaded into target brain tissue. Additionally, NC sensitivity to FUS allowed for the use of FUS as a way to release NC load with temporal control. This is referred to as release-FUS.

FUS BBB opening

The reliability of FUS BBBO as a localized delivery method was tested by targeting both the anterior cingulate cortex (ACC) (n=5) and the hippocampus (n=9) with FUS 5 minutes after EBD IV injection. Immediately following FUS BBBO, 0.1mL/ kg of Gadovist MRI contrast agent was injected IV. Animals were first pre scanned at 9.4T, then MR imaged at 15 and 30 minutes following the FUS procedure. Enhanced T_1-weighted MRI contrast was evident in both brain regions indicating that the BBB was opened, allowing Gadovist contrast to locally extravasate into the FUS targeted region (Figure 2a,c, f and g). The region of BBB opening, evident by EBD, could also be seen upon removal of the perfused brain tissue both in the ACC (Figure 2b) and the hippocampus(Figure 2e). Note that the hippocampus is a deeper brain structure providing a more faint EBD appearance compared to the more superficial ACC target. BBBO was further confirmed by EBD fluorescence (excitation at 620nm, emission at 680nm) in 10μm brain sections from FUS treated animals (Figure 2, d and h).

Localized nanocluster delivery with FUS induced BBB opening

To investigate whether NCs could be locally deposited into the hippocampus using FUS BBBO, animals were first prescanned by MRI at 9.4T, and then injected with EBD by tail vein catheter. FUS BBB opening was then carried out, as described above, in the absence of injected Gadovist. Immediately afterwards, 2 mL/kg of HEPES buffer solution containing NCs (2 mg/mL) was injected into the rat by IV. Animals were then MR imaged again at 9.4T 15 minutes, 30 minutes and 1 hour after NC injection. Control animals underwent the same BBBO procedure but received a saline injection without NCs. ROIs of target hippocampi and off target hippocampi were collected, and the MR images are shown in Figure 3a. The top row of images were taken from a

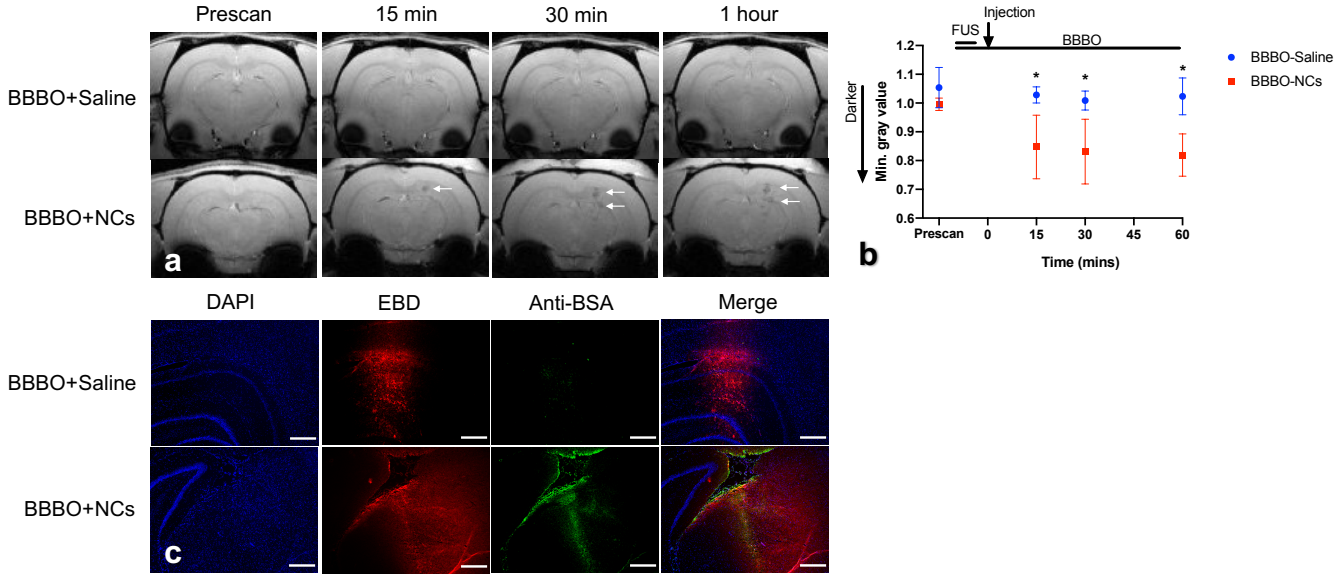

Figure 3. Nanoclusters load into brain tissue after localized BBB opening. (a) T1-weighted MR images of an animal treated with saline (top) or NCs (bottom) following BBB opening in the hippocampus. NCs provide increasing MRI contrast as they load into brain tissue at 15, 30 mins and 1hr after injection (white arrows). (b) Plotted MRI minimum gray values from hippocampal ROIs before and at 15 min, 30 min and 1hr after FUS BBB opening and NC (red) or saline (blue) injection(Time 0). (c) Immunofluorescence staining with antibody to BSA showing NC distribution compared to EBD or rat serum albumin (EBD-RSA) distribution in animal treated with unloaded-NCs (bottom) or saline (top) after BBB opening.

control animal before, 15 minutes, 30 minutes, and 1 hour after saline injection, and the bottom row of images were taken from an animal before and after NC injection. The white arrows in Figure 3a point to regions where enhanced MR contrast was observed in NC treated animals. Minimum gray values in the ROIs were analyzed using FIJI by ImageJ, and the results are plotted in Figure 3b. MRI contrast was enhanced in animals who received NCs compared to animals who received only saline following FUS BBBO. Figure 3c shows representative immunofluorescence microscopy images taken from animals treated with NCs (bottom row) and from control animals injected with saline (top row). DAPI staining made visible the cell distribution in the tissue section, and EBD fluorescence showed areas of BBBO. BSA staining revealed that NCs were present in areas of brain tissue where the BBB had been opened. Furthermore, no abnormal glial cell morphology was observed from NC loaded and FUS treated rats compared to sham animals. The results show that targeted and spatially-restricted entry of NCs into the brain can be achieved through FUS-induced BBBO.

FUS stimulated release of dye from nanoclusters

To test whether NCs could release their load in vivo with release-FUS, animals first underwent BBB opening targeted to either the right or left hippocampus. The BBBO procedure was immediately followed by IV injection of either FITC-loaded NCs or unloaded-NCs. A small group of FITC-NC treated animals (n=3) were sacrificed at 15 minutes post injection to observe any immediate natural FITC release from NCs. Figure 4 illustrates the timeline of procedures used on all other animals. MR images were acquired 15 minutes and 30 minutes post injection to confirm NC loading into target brain tissue. Following the 30 minute scan, animals received a release-FUS

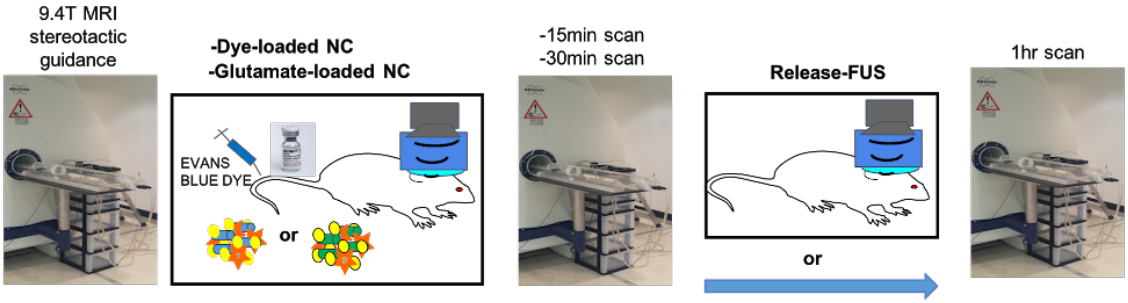

Figure 4. FUS-induced BBBO and release-FUS procedure. Animals were MRI prescanned at 9.4T in a stereotaxic frame and hippocampal coordinates were measured. Animals then underwent BBB opening procedure followed by injection of dye-loaded NCs or unloaded NCs. Rats were MR imaged at 15 and 30 minutes after NC injection. They were then either treated with a release-FUS treatment or not and MR imaged again at 1hr post injection.

treatment and were MR imaged again at 1 hour post injection. Control animals received the same treatments but were not exposed to a release-FUS. Animals were then sacrificed at 90 minutes post NC injection for fluorescent microscopy analysis of FITC dye in the BBBO region evident by EBD fluorescence.

The top row of Figure 5a shows fluorescence images of brain tissue sections taken from animals that received no release-FUS, and the bottom row shows results from those that received the release-FUS treatment. Little to no FITC dye fluorescence was seen at 15 minutes post injection (not shown), indicating that NCs remain stable after loading into brain tissue without releasing their contents. At 90 minutes post injection, FITC dye fluorescence in the target hippocampus of animals that received FITC-NCs was not significantly different from animals who were treated with unloaded NCs. Release-FUS treatment, however, significantly increased the number of FITC particles that were detected in FITC-NC injected animals by immunofluorescence analysis, as seen in the tissue section at the bottom of Figure 5a. Figure 5b summarizes the FITC dye analysis, where the number of FITC particles detected in tissue sections is shown for the various experimental groups. Animals injected with unloaded NCs exhibited the lowest FITC particle count. FITC counts from animals injected with FITC loaded NCs 15 minutes and 1 hour before sacrifice were also relatively low. Animals that received FITC-NCs followed by release-FUS treatments, however, exhibited significantly increased levels of FITC particles in tissue sections. These results indicate that release-FUS can trigger release of NC load in vivo.

Release of glutamate from NCs causes modulation cFos activation in target tissue

The procedure diagrammed in Figure 4 was repeated with glutamate-loaded nanoclusters (Glu-NCs) to test whether drug loaded NCs could cause localized changes in brain activity. Glu-NCs were injected immediately after FUS BBB opening in either the left or right hippocampus. NC deposition in target brain areas was confirmed with MRI 15 and 30 minutes following NC injection, and release-FUS was applied after the 30 minute scan. Animals were then MR imaged again and sacrificed at 90 minutes post release-FUS or 2 hours after NC injection. Figure 6a shows immunofluorescence microscopy images taken of tissue from animals that received unloaded NCs and Glu-NCs. The area of BBBO can be seen with EBD fluorescence, and there was robust cFos activation in animals that received Glu-NCs. The results demonstrate that

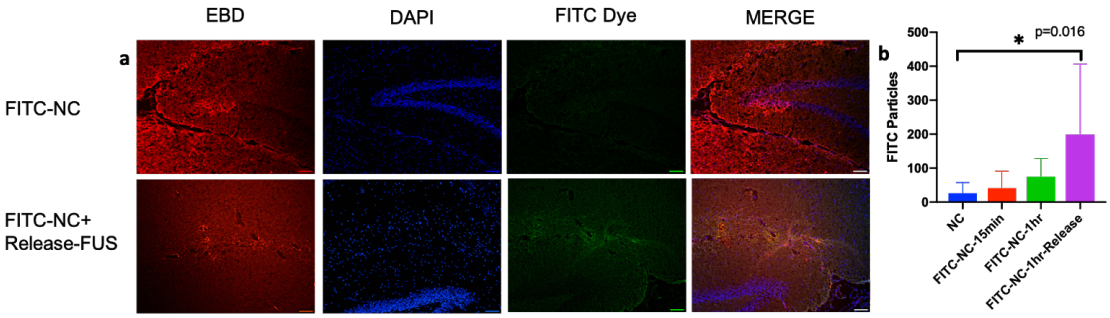

Figure 5. Dye release from NCs in vivo with release-FUS. (a) Immunofluorescence analysis of brain tissue sections from animals sacrificed 90 minutes post injection. (top row) Representative immunofluorescence images of hippocampi 90 minutes post dye-loaded NC injection and (bottom row) 90 minutes post dye-NC injection + Release FUS. Scale bar: 100μm. (b) FITC particle quantification revealed a significant difference in numbers of FITC particles between FITC-NC-1hr-Release and unloaded NC groups. No other significant differences were found between groups.

glutamate was released at sufficient levels to activate neural circuits in vivo. As a control, FUS was applied to open the BBB but no NCs were injected. Figure 5b summarizes the cFos microscopy results. There was no increase in cFos staining in areas of BBBO compared to sham animals, verifying lack of neural activation from BBBO alone. This is consistent with previous studies indicating that the FUS parameters used to open BBB does not modulate neural activity [31,32]. Additional control experiments in separate animals were conducted to ensure that the addition of a release-FUS was not causing cFos activation. These animals received the same BBBO and release-FUS procedure but instead of Glu-NCs received either a saline injection or unloaded NCs (data not shown). There was no significant difference in cFos expression between these groups and the BBB opening alone group, as seen in Figure 6b. Together, these data demonstrate that glutamate delivery to brain tissue via FUS-mediated BBBO and NC release is able to produce localized neuromodulation.

Discussion

The BBB is generally an impediment to the delivery of therapeutic agents. FUS has gained attention as a tool for focal BBB opening[4,6–10,20] and can penetrate the skull to safely open the BBB at specific locations providing transient BBB permeability lasting 4 to 6 hours, after which the BBB resumes normal functioning [16] [35] [36] [12,16]. We investigated the use of FUS for non-invasive neuromodulation by combining FUS-induced BBBO and nanocluster drug delivery. The method presented takes advantage of the BBB by using FUS BBBO to localize delivery of glutamate for spatially specific neuromodulation [5,15,33–35]. Our most important finding is that ultrasound-triggered glutamate release from nanoclusters in vivo can increase neural activity, as measured with increased cFOS staining. This demonstrates that the amount of nanocluster entry into the brain and release of drug from the clusters are sufficient to have neuromodulatory effects, demonstrating feasibility of this method for localized drug delivery. Our results show that cFOS levels are not altered with either application of BBB-FUS alone or BBB-FUS and release-FUS, verifying lack of neural activation by low power FUS, as previously shown(1,2).

FUS BBB opening did not cause heightened GFAP expression. This supports previous studies highlighting either no inflammatory response or a brief transient inflammatory response following BBB opening [37,38]. In addition, the use of

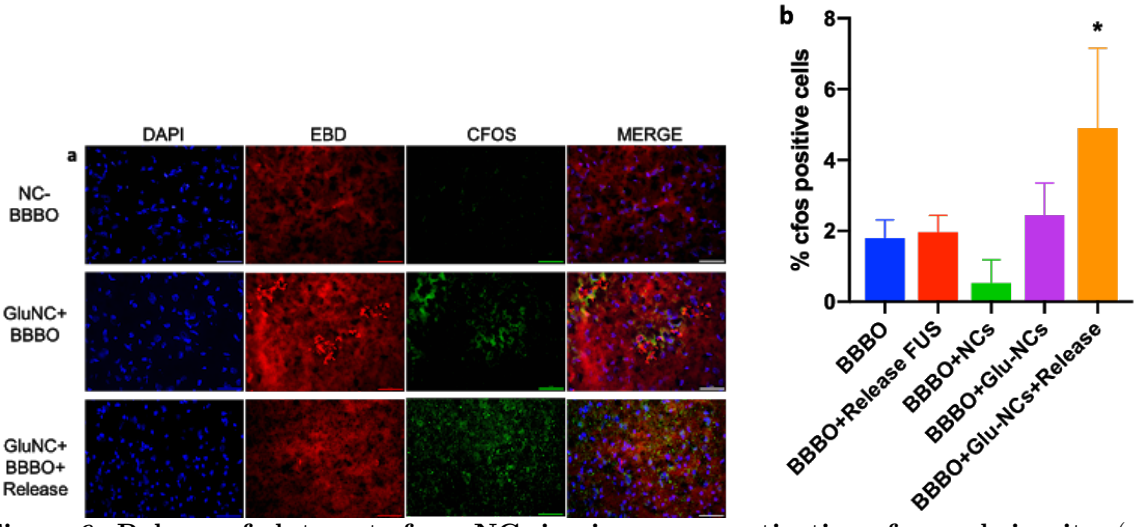

Figure 6. Release of glutamate from NCs in vivo causes activation of neural circuits. (a) Immunofluorescence staining for cFos 2hrs following either unloaded NC (top) or glutamate-loaded NC delivery (middle and bottom rows) to the brain with FUS BBB opening. Animals that did not receive a release-FUS treatment (middle row) showed a very localized c-Fos expression while animals who received a release-FUS treatment showed a more robust and diffuse c-Fos expression (bottom row). Control tissue (BBBO-unloaded NCs) displayed very little c-Fos expression (top row). Scale bar 50um. (b) Percent c-Fos positive cells were significantly higher in animals who received Glu-loaded NCs with a Release-FUS treatment compared to all other groups (p¡0.05).

albumin-based drug carriers have previously been shown to be safe to administer IV [21,39–44] [21], and our work showed no clear additional inflammatory response or cellular toxicity with the presence of albumin NCs in the brain [42,45]. The presence of NCs in brain regions that were not targeted for BBB opening was also not observed. Similarly, cellular-intracellular uptake of NCs could be observed, which is consistent with previous studies of NCs with similar nanoparticle composition [45].

A major advantage compared to systemic drug delivery is that FUS-mediated delivery can be used to treat of symptoms originating in specific brain regions while avoiding side effects caused by neuromodulation in other areas. Combining BBBO with albumin-based NCs allows for current clinical drugs to be used in novel temporally and spatially specific ways while limiting off target effects. Additionally, this method can enable the research and use of drugs that do not normally cross the BBB.

To make the NCs MRI visible, our collaborator Dr. Yuping Bao has developed ultrasmall iron oxide-based contrast agents. Nanoparticle-based T1 MRI contrast agents have become increasingly attractive markers for drug delivery [46] [47] [45] [25,26,48]. Our recent paper demonstrates that by themselves, the ultrasmall iron oxide nanoparticles are cleared from the blood quickly through the kidneys[25,49]. However, we demonstrated that the use of cross-linked BSA increases the overall hydrodynamic radius and substantially improves circulation time to ¿2 hours[25]. Furthermore, we were able to encapsulate both a fluorescent dye and an antibody [25] indicating the versatility of our NC. Stability of the NCs is important to effectively deliver the imaging probes and drugs to the BBBO site and to prevent the release of agents into the bloodstream during circulation. Glutaraldehyde cross-linking was used to provide this stability [25], and we have shown that the NCs are stable in vitro and in vivo [25]. Importantly, the degradation rate and baseline drug release rates of the NCs can be adjusted by changing the degree of glutaraldehyde cross-linking. Increased cross-linking

will improve stability and reduce baseline release [50]. The MRI visibility of this drug carrier can provide independent validation of the site of neuromodulation and avoids the circularity of using the neuromodulatory effect to verify the location of delivery.

The use of FUS BBBO for non-invasive, location-specific drug delivery has high potential as a method to both treat and investigate neurological disorders. However, complications with pre-clinical applications arise due to the need to use anesthesia for the MRI-guided FUS procedure. This requires the animal to recover from anesthesia prior to any behavioral studies, creating confounds with timing of drug action and behavioral outcomes. The use of NCs allows release of drugs at a later time following the BBBO procedure, enabling the pairing of drug release following anesthesia recovery in a behaving animal. The sensitivity of the albumin-based particles to FUS is consistent with previous studies and has been harnessed for drug delivery strategies [24]. Our group has future plans to apply release-FUS via a wearable transducer enabling temporal specific drug release in behaving animals. This method replaces focal injections, drug delivery by cannula, or implantation of osmotic minipumps, all of which are invasive, cause tissue damage, and are challenging to use for deeper brain regions. The method is intentionally based on techniques and materials already used in humans, and can therefore be readily adaptable for use in humans. If widely used, FUS-mediated drug delivery could help bridge the gap between preclinical studies and clinical use because the same technique would be used in both animals and humans.

Conclusions

Glutamate loaded, albumin based NCs were able to load into brain tissue with FUS BBBO and provided enough MRI contrast to confirm location in target brain region. Glutamate release from NCs was able to cause neuronal activation, evidenced by enhanced cFos expression, indicating that NCs can load enough drug or neuromodulator to cause changes in neuronal activity.

This new method of non-invasive, location-specific drug delivery could potentially replace focal injections, drug delivery by cannula, or implantation of osmotic minipumps, all of which are invasive, cause tissue damage, and are challenging to use for deeper brain regions. The method is intentionally based on techniques and materials already used in humans, and can therefore be readily adaptable for use in humans. If widely used, FUS-mediated drug delivery could help bridge the gap between preclinical studies and clinical use because the same technique would be used in both animals and humans.

Acknowledgments

This research was supported in part by an NSF EPSCoR Research Infrastructure grant to Clemson University (1632881). The authors gratefully acknowledge use of the services and facilities of the University of Alabama at Birmingham Small Animal Imaging Shared Facility.

References

1. T.R. Insel, S.C. Landis, Twenty-five years of progress: the view from NIMH and NINDS., Neuron. 80 (2013) 561–567. doi:10.1016/j.neuron.2013.09.041.

2. K. Krug, C.D. Salzman, S. Waddell, Understanding the brain by controlling neural activity., Philos Trans R Soc Lond, B, Biol Sci. 370 (2015) 20140201. doi:10.1098/rstb.2014.0201.

3. X. Jiang, J. Nardelli, Cellular and molecular introduction to brain development., Neurobiol. Dis. 92 (2016) 3–17. doi:10.1016/j.nbd.2015.07.007.

4. J.J. Choi, S. Wang, Y.-S. Tung, B. Morrison, E.E. Konofagou, Molecules of various pharmacologically-relevant sizes can cross the ultrasound-induced blood-brain barrier opening in vivo., Ultrasound Med. Biol. 36 (2010) 58–67. doi:10.1016/j.ultrasmedbio.2009.08.006.

5. C. Bing, M. Ladouceur-Wodzak, C.R. Wanner, J.M. Shelton, J.A. Richardson, R. Chopra, Trans-cranial opening of the blood-brain barrier in targeted regions using a stereotaxic brain atlas and focused ultrasound energy., J. Ther. Ultrasound. 2 (2014) 13. doi:10.1186/2050-5736-2-13.

6. P.-C. Chu, W.-Y. Chai, C.-H. Tsai, S.-T. Kang, C.-K. Yeh, H.-L. Liu, Focused Ultrasound-Induced Blood-Brain Barrier Opening: Association with Mechanical Index and Cavitation Index Analyzed by Dynamic Contrast-Enhanced Magnetic-Resonance Imaging., Sci. Rep. 6 (2016) 33264. doi:10.1038/srep33264.

7. S. Meairs, A. Alonso, Ultrasound, microbubbles and the blood-brain barrier., Prog. Biophys. Mol. Biol. 93 (2007) 354–362. doi:10.1016/j.pbiomolbio.2006.07.019.

8. C. Bing, M. Ladouceur-Wodzak, C.R. Wanner, J.M. Shelton, J.A. Richardson, R. Chopra, Trans-cranial opening of the blood-brain barrier in targeted regions using a stereotaxic brain atlas and focused ultrasound energy., J. Ther. Ultrasound. 2 (2014) 13. doi:10.1186/2050-5736-2-13.

9. J. Xia, P.-H. Tsui, H.-L. Liu, Low-Pressure Burst-Mode Focused Ultrasound Wave Reconstruction and Mapping for Blood-Brain Barrier Opening: A Preclinical Examination., Sci. Rep. 6 (2016) 27939. doi:10.1038/srep27939.

10. E. Thévenot, J.F. Jordão, M.A. O'Reilly, K. Markham, Y.-Q. Weng, K.D. Foust, et al., Targeted delivery of self-complementary adeno-associated virus serotype 9 to the brain, using magnetic resonance imaging-guided focused ultrasound., Hum. Gene Ther. 23 (2012) 1144–1155. doi:10.1089/hum.2012.013.

11. T. Nhan, A. Burgess, E.E. Cho, B. Stefanovic, L. Lilge, K. Hynynen, Drug delivery to the brain by focused ultrasound induced blood-brain barrier disruption: quantitative evaluation of enhanced permeability of cerebral vasculature using two-photon microscopy., J. Control. Release. 172 (2013) 274–280. doi:10.1016/j.jconrel.2013.08.029.

12. A. Burgess, K. Shah, O. Hough, K. Hynynen, Focused ultrasound-mediated drug delivery through the blood-brain barrier., Expert Rev. Neurother. 15 (2015) 477–491. doi:10.1586/14737175.2015.1028369.

13. J.J. Choi, M. Pernot, S.A. Small, E.E. Konofagou, Noninvasive, transcranial and localized opening of the blood-brain barrier using focused ultrasound in mice., Ultrasound Med. Biol. 33 (2007) 95–104. doi:10.1016/j.ultrasmedbio.2006.07.018.

14. C. Bing, Y. Hong, C. Hernandez, M. Rich, B. Cheng, I. Munaweera, et al., Characterization of different bubble formulations for blood-brain barrier opening using a focused ultrasound system with acoustic feedback control., Sci. Rep. 8 (2018) 7986. doi:10.1038/s41598-018-26330-7.

15. G. Samiotaki, M.E. Karakatsani, A. Buch, S. Papadopoulos, S.Y. Wu, S. Jambawalikar, et al., Pharmacokinetic analysis and drug delivery efficiency of the focused ultrasound-induced blood-brain barrier opening in non-human primates., Magn. Reson. Imaging. 37 (2017) 273–281. doi:10.1016/j.mri.2016.11.023.

16. C. Poon, D. McMahon, K. Hynynen, Noninvasive and targeted delivery of therapeutics to the brain using focused ultrasound., Neuropharmacology. 120 (2017) 20–37. doi:10.1016/j.neuropharm.2016.02.014.

17. N. Lipsman, M.L. Schwartz, Y. Huang, L. Lee, T. Sankar, M. Chapman, et al., MR-guided focused ultrasound thalamotomy for essential tremor: a proof-of-concept study., Lancet Neurol. 12 (2013) 462–468. doi:10.1016/S1474-4422(13)70048-6.

18. N. Lipsman, Y. Meng, A.J. Bethune, Y. Huang, B. Lam, M. Masellis, et al., Blood-brain barrier opening in Alzheimer's disease using MR-guided focused ultrasound., Nat. Commun. 9 (2018) 2336. doi:10.1038/s41467-018-04529-6.

19. T. Mainprize, N. Lipsman, Y. Huang, Y. Meng, A. Bethune, S. Ironside, et al., Blood-Brain Barrier Opening in Primary Brain Tumors with Non-invasive MR-Guided Focused Ultrasound: A Clinical Safety and Feasibility Study., Sci. Rep. 9 (2019) 321. doi:10.1038/s41598-018-36340-0.

20. K.-T. Chen, K.-C. Wei, H.-L. Liu, Theranostic Strategy of Focused Ultrasound Induced Blood-Brain Barrier Opening for CNS Disease Treatment., Front. Pharmacol. 10 (2019) 86. doi:10.3389/fphar.2019.00086.

21. A. Loureiro, N.G. Azoia, A.C. Gomes, A. Cavaco-Paulo, Albumin-Based Nanodevices as Drug Carriers., Curr. Pharm. Des. 22 (2016) 1371–1390. doi:10.2174/1381612822666160125114900.

22. M.T. Larsen, M. Kuhlmann, M.L. Hvam, K.A. Howard, Albumin-based drug delivery: harnessing nature to cure disease., Mol. Cell. Ther. 4 (2016) 3. doi:10.1186/s40591-016-0048-8.

23. G. Wang, J. Liu, S. Lü, Y. Lü, C. Guo, D. Zhao, et al., Ultrasonic destruction of albumin microbubbles enhances gene transfection and expression in cardiac myocytes., Chin. Med. J. 124 (2011) 1395–1400.

24. T.-Y. Liu, M.-Y. Wu, M.-H. Lin, F.-Y. Yang, A novel ultrasound-triggered drug vehicle with multimodal imaging functionality., Acta Biomater. 9 (2013) 5453–5463. doi:10.1016/j.actbio.2012.11.023.

25. J. Sherwood, M. Rich, K. Lovas, J. Warram, M.S. Bolding, Y. Bao, T1-Enhanced MRI-visible nanoclusters for imaging-guided drug delivery., Nanoscale. 9 (2017) 11785–11792. doi:10.1039/c7nr04181k.

26. J. Sherwood, K. Lovas, M. Rich, Q. Yin, K. Lackey, M.S. Bolding, et al., Shape-dependent cellular behaviors and relaxivity of iron oxide-based T1 MRI contrast agents., Nanoscale. 8 (2016) 17506–17515. doi:10.1039/c6nr06158c.

27. F.-Y. Yang, W.-M. Fu, W.-S. Chen, W.-L. Yeh, W.-L. Lin, Quantitative evaluation of the use of microbubbles with transcranial focused ultrasound on blood-brain-barrier disruption., Ultrason. Sonochem. 15 (2008) 636–643. doi:10.1016/j.ultsonch.2007.08.003.

28. A. Fedorov, R. Beichel, J. Kalpathy-Cramer, J. Finet, J.-C. Fillion-Robin, S. Pujol, et al., 3D Slicer as an image computing platform for the Quantitative Imaging Network., Magn. Reson. Imaging. 30 (2012) 1323–1341. doi:10.1016/j.mri.2012.05.001.

29. N.J. Tustison, B.B. Avants, P.A. Cook, Y. Zheng, A. Egan, P.A. Yushkevich, et al., N4ITK: improved N3 bias correction., IEEE Trans. Med. Imaging. 29 (2010) 1310–1320. doi:10.1109/TMI.2010.2046908.

30. J. Schindelin, I. Arganda-Carreras, E. Frise, V. Kaynig, M. Longair, T. Pietzsch, et al., Fiji: an open-source platform for biological-image analysis., Nat. Methods. 9 (2012) 676–682. doi:10.1038/nmeth.2019.

31. N. McDannold, Y. Zhang, C. Power, C.D. Arvanitis, N. Vykhodtseva, M. Livingstone, Targeted, noninvasive blockade of cortical neuronal activity., Sci. Rep. 5 (2015) 16253. doi:10.1038/srep16253.

32. N. McDannold, C.D. Arvanitis, N. Vykhodtseva, M.S. Livingstone, Temporary disruption of the blood-brain barrier by use of ultrasound and microbubbles: safety and efficacy evaluation in rhesus macaques., Cancer Res. 72 (2012) 3652–3663. doi:10.1158/0008-5472.CAN-12-0128.

33. N. Nainwal, Recent advances in transcranial focused ultrasound (FUS) triggered brain delivery., Curr. Drug Targets. 18 (2017) 1225–1232. doi:10.2174/1389450117666161222160025.

34. Y. Zhang, H. Tan, E.H. Bertram, J.-F. Aubry, M.-B. Lopes, J. Roy, et al., Non-Invasive, Focal Disconnection of Brain Circuitry Using Magnetic Resonance-Guided Low-Intensity Focused Ultrasound to Deliver a Neurotoxin., Ultrasound Med. Biol. 42 (2016) 2261–2269. doi:10.1016/j.ultrasmedbio.2016.04.019.

35. H. Chen, C.C. Chen, C. Acosta, S.-Y. Wu, T. Sun, E.E. Konofagou, A new brain drug delivery strategy: focused ultrasound-enhanced intranasal drug delivery., PLoS ONE. 9 (2014) e108880. doi:10.1371/journal.pone.0108880.

36. M. Thanou, W. Gedroyc, MRI-Guided Focused Ultrasound as a New Method of Drug Delivery., J. Drug Deliv. 2013 (2013) 616197. doi:10.1155/2013/616197.

37. D. McMahon, R. Bendayan, K. Hynynen, Acute effects of focused ultrasound-induced increases in blood-brain barrier permeability on rat microvascular transcriptome., Sci. Rep. 7 (2017) 45657. doi:10.1038/srep45657.

38. H.-C. Tsai, C.-H. Tsai, W.-S. Chen, C. Inserra, K.-C. Wei, H.-L. Liu, Safety evaluation of frequent application of microbubble-enhanced focused ultrasound blood-brain-barrier opening., Sci. Rep. 8 (2018) 17720. doi:10.1038/s41598-018-35677-w.

39. F. Kratz, Albumin as a drug carrier: design of prodrugs, drug conjugates and nanoparticles., J. Control. Release. 132 (2008) 171–183. doi:10.1016/j.jconrel.2008.05.010.

40. R. Naveen, K. Akshata, S. Pimple, P. Chaudhari, R. Naveen, K. Akshata, et al., A review on albumin as drug carrier in treating different diseases and disorders, (n.d.).

41. Bairagi, Mittal, Mishra, Bairagi, Mittal, Mishra, Albumin: A Versatile Drug Carrier, (n.d.).

42. W. Lohcharoenkal, L. Wang, Y.C. Chen, Y. Rojanasakul, Protein nanoparticles as drug delivery carriers for cancer therapy., Biomed Res. Int. 2014 (2014) 180549. doi:10.1155/2014/180549.

43. Z. Liu, X. Chen, Simple bioconjugate chemistry serves great clinical advances: albumin as a versatile platform for diagnosis and precision therapy., Chem. Soc. Rev. 45 (2016) 1432–1456. doi:10.1039/c5cs00158g.

44. D. Gil, A. Frank-Kamenetskii, J. Barry, V. Reukov, Y. Xiang, A. Das, et al., Albumin-Assisted Method Allows Assessment of Release of Hydrophobic Drugs From Nanocarriers., Biotechnol. J. 13 (2017). doi:10.1002/biot.201700337.

45. D. Shi, G. Mi, S. Bhattacharya, S. Nayar, T.J. Webster, Optimizing superparamagnetic iron oxide nanoparticles as drug carriers using an in vitro blood-brain barrier model., Int. J. Nanomedicine. 11 (2016) 5371–5379. doi:10.2147/IJN.S108333.

46. W. He, F. Yang, Y. Wu, S. Wen, P. Chen, Y. Zhang, et al., Microbubbles with surface coated by superparamagnetic iron oxide nanoparticles, Mater. Lett. 68 (2012) 64–67. doi:10.1016/j.matlet.2011.10.013.

47. Y. Xu, Y. Qin, S. Palchoudhury, Y. Bao, Water-soluble iron oxide nanoparticles with high stability and selective surface functionality., Langmuir. 27 (2011) 8990–8997. doi:10.1021/la201652h.

48. X. Cai, F. Yang, N. Gu, Applications of magnetic microbubbles for theranostics., Theranostics. 2 (2012) 103–112. doi:10.7150/thno.3464.

49. F. Alexis, E. Pridgen, L.K. Molnar, O.C. Farokhzad, Factors affecting the clearance and biodistribution of polymeric nanoparticles., Mol. Pharm. 5 (2008) 505–515. doi:10.1021/mp800051m.

50. C. Weber, J. Kreuter, K. Langer, Desolvation process and surface characteristics of HSA-nanoparticles., Int. J. Pharm. 196 (2000) 197–200. doi:10.1016/S0378-5173(99)00420-2.